EUROPEAN FUSION DEVELOPMENT AGREEMENT

EFDA–JET–PR(05)-21

Ph. Lauber, S. Günter, S.D. Pinches
and JET EFDA contributors

Kinetic Properties of Shear Alfvén Eigenmodes in Tokamak Plasmas

Kinetic Properties of Shear Alfvén Eigenmodes in Tokamak Plasmas

Ph. Lauber[1], S. Günter[1], S.D. Pinches[1]
and JET EFDA contributors*

[1]Max-Planck-Institut f¨ ur Plasmaphysik, EURATOM Assoz iation, Boltz mannstr. 2, D-85748 Garching
** See annex of J. Pamela et al, "Overview of JET Results ",*
(Proc. 20th IAEA Fusion Energy Conference, Vilamoura, Portugal (2004).

Preprint of Paper to be submitted for publication in
Physics of Plasmas

ABSTRACT

This work reports on numerical calculations concerning the kinetic properties of low-*n*, low-*m* toroidal Alfvén eigenmodes (TAEs) in tokamak plasmas for fusion relevant parameters. The selfconsistent and non-perturbative code Ligka [Ph. Lauber, Ph.D. Thesis, TU München, (2003)] is employed. It is based on a linear gyro-kinetic model consisting of the quasi-neutrality equation and the moment equation for the perturbed current. It is shown that in a certain limit the underlying equations of Ligka can be simplified to the equations known as the 'reduced kinetic model'.

An antenna-like version of Ligka allows one to systematically find all shear-Alfvén-type modes in a given frequency interval, such as kinetic TAEs (KTAEs) and kinetically modified TAEs. The coupling to the kinetic Alfvén wave (KAW) is found in the form of continuum damping and radiative damping. For the cases examined here, no mode conversion in the centre is found. In the case of a large non-ideal parameter, damping rates around 0.5 - 1% are found, close to experimental measurements.

1. INTRODUCTION

The stability properties of the toroidal Alfvén eigenmode (TAE) [1, 2] in magnetically confined fusion plasmas are of great interest because TAEs can be driven unstable by fusion-born α-particles with dangerous consequences for the overall plasma stability and confinement [3]. In order to make predictions for an ignited plasma, as expected in the International Tokamak Experimental Reactor (ITER), the background damping mechanisms of TAEs have to be carefully investigated. These mechanisms are electron and ion Landau damping, continuum damping, collisional damping and radiative damping. The latter mechanism requires a non-perturbative description, since the MHD properties of the mode structure are modified by coupling to the kinetic Alfvén wave (KAW) [4].

The application of perturbative, fluid models like Castor-K [5] and Nova-K [6] to the Joint European Torus (JET) for low-n, low-m cases resulted in damping rates which were too small by one order of magnitude compared to the measured damping rates [7, 8]. With a gyro-kinetic, perturbative extension of Castor-K based on a complex resistivity model [9], considerably higher damping rates with a discrepancy of a factor of 2 were calculated, verifying the importance of mode conversion of Alfvén and kinetic Alfvén eigenmodes. The global gyro-kinetic wave code Penn [10] found agreement with the experiment, proposing mode conversion in the plasma centre as the main damping mechanism. However, there has been no confirmation of this mechanism by analytical estimates or other codes such as Castor-K. Indeed, recent work on this topic, employing a global, reduced kinetic model [11] also did not confirm any significant mode conversion mechanism in the centre. Instead, continuum damping near the plasma edge was found to be important, leading to damping rates comparable to the experiment.

The aim of this paper is to carry out numerical calculations not only on this open question but also on the properties of kinetic TAEs (KTAEs) using the gyro-kinetic, linear eigenvalue code Ligka [12]. This code is based on a self-consistent model developed by Qin *et al.* [13, 14] consisting

of the quasi-neutrality equation and the moment equation for the perturbed current. It is non-perturbative, since it allows for a non-linear dependence of the eigenvalue through the velocity space integrals and also for a mode structure which is not prescribed by ideal MHD calculations. The propagator integrals along the drift orbits of ions and electrons are carried out numerically using the drift-kinetic code Hagis [15, 16]. The resonance integrals are accurately solved by employing rational interpolation and grid refinement techniques. The Ligka model therefore encompasses all of the damping mechanisms mentioned above, except collisional damping, which is assumed to be small compared to the other types of damping. It will however, be included in a future version of the code.

The remainder of this paper is organised as follows: In Section II basic quantities are defined and it is shown that the underlying equations of Ligka can be simplified to the 'reduced kinetic model' as used in [11] and [17] proving their validity in the regime under investigation. Section 3 describes a new mode of operation of Ligka, allowing the code to model an external driving antenna in a simple way. This extension enables one to systematically find all (stable) modes in a given frequency range. Section 4 presents results on TAEs and KTAEs modified by coupling to the KAW by continuum damping and radiative damping. Damping rates for open and closed gap cases are given. The paper finishes with conclusions and an outlook.

2. BASICS AND EQUATIONS

The first comprehensive description of TAEs can be found in Ref. [1, 2], where it was shown analytically and numerically how toroidal geometry breaks up the continuous Alfvén spectra of a cylindrical plasma, generates gaps and permits global modes within these gaps.

The gap frequency corresponding to two poloidal mode numbers m and $m + 1$ and the toroidal mode number n can be estimated from the condition for the two corresponding parallel components of the wave vectors $k_m(r) = [nq(r) - m]/Rq(r)$ and k_m:

$$k_m(r) = -k_{m+1}(r) \tag{1}$$

which leads to

$$q_m = q(r_m) = \frac{m + 1/2}{n} \quad and \quad \frac{\omega^2}{\omega^2_A} = \frac{n}{2m + 1} \tag{2}$$

where R is the major radius of the plasma and $q(r)$ the safety factor. This relation defines r_m, the radial position of the gap. v_A is the on-axis Alfvén velocity and $w_A = v_A/R$.

The gap width (in frequency) is of the same order as the inverse aspect ratio $\epsilon = r/R$. The TAE

itself is located within this gap. Its exact frequency depends on the magnetic shear s = $rq'(r)/q(r)$: in the zero-shear limit it sits on the low-frequency boundary, for $s \to \infty$ on the high-frequency side[2].

The dispersion relation for a low-β, small $\in$ circular tokamak plasma can be described by a three term recursion relation given for high-n in Refs. [18{20], for low-shear cases in [21], and for arbitrary n-numbers in [17].

The inclusion of non-ideal effects, namely parallel electric fields and finite ion gyro-radii, leads to significant changes of the TAE modes and generates a new set of modes, the kinetic TAEs (KTAEs) and a new type of damping, called radiative damping or 'tunnelling' [4, 17]. They are quantified by the non-ideal parameter

$$\lambda = \frac{4ms\rho_i}{r_m \in^{3/2}} \sqrt{\frac{3}{4} + \frac{T_e}{T_i}} \tag{3}$$

with $\rho_i = v_{thi}/w_{ci}$ being the ion gyro-radius, $v_{th} = \sqrt{T/m}$ the particles' thermal velocity, w_c the cyclotron frequency and $\hat{\in}^{3/2} = 5r_m/2R$. Analytical expressions for the non-ideal, arbitrary-n dispersion relation can be derived for a circular-cross-section in the low-β-limit again in the form of a three term recursion relation [17].

The following basic equation is employed in the latter reference as the relevant one for non-ideal shear Alfvén modes:

$$\nabla_\perp \left(\frac{\omega^2}{\upsilon_A^2} \nabla_\perp \phi \right) + \frac{\partial}{\partial s} \nabla_\perp^2 \frac{\partial \phi}{\partial s} = \delta_s^2 \left(\frac{\omega}{c} \nabla_\perp^4 \frac{\partial A_{/\!/}}{\partial s} - \frac{3}{4} \frac{\omega^2}{\upsilon_A^2} \rho_i^2 \nabla_\perp^4 \frac{\partial A_{/\!/}}{\partial s} \right) \tag{4}$$

It is derived from the vorticity equation with finite Larmor radius (FLR) corrections and Ohm's law as given in Ref. [22, 23]. Here, ϕ is the electrostatic potential, $A_{||}\mathbf{b}$ the magnetic vector potential, r the radial coordinate and s the coordinate along the field line. δ_s is the skin depth $\delta_s = c^2 \in_0 / w\sigma$ with σ being the parallel complex electrical conductivity, which was chosen to be $\sigma/\in_0 = iw^2_{pe}/(w + iv_{eff} - k^2_{||} v^2_{the}/w)$. w_{pe} and v_{eff} are the electron plasma frequency and the effective electron collision frequency respectively.

Near the singular layer of the ideal MHD equation (left hand side of Eq.4), the right hand side becomes most important and by using the ansatz

$$\phi = \sum_m \phi_m e^{i(n\varphi - m\theta - \omega t)} \tag{5}$$

for the perturbed quantities it can be simplified by the substitutions $iwA_{||}/c \rightarrow \partial\phi/\partial s$, $\partial/\partial s \rightarrow ik_{||} \equiv i\,(n\text{-}m/q(r))\,/R$, $w^2/w^2_A \equiv \Omega^2 = \Omega^2_m \equiv 1/4q^2_m$ to yield a coupled system of fourth-order differential equations with the right hand side reducing to

$$-r^2_{LT}\,\Omega^2_m \frac{\partial^4 \phi_m}{\partial r^4} \tag{6}$$

with

$$r^2_{LT} = \frac{3}{4}\,\rho^2_i = \rho^2_s = \rho^2_i \left\{ \frac{3}{4} + \frac{T_e}{T_i}\left[1 + \frac{v^2_A}{v^2_{the}}\,(1 + \frac{\nu_{eff}}{|k_{||}|v_A})\right]\right\}, \tag{7}$$

The underlying equations of Ligka (derived in [13, 14]) consist of the quasi-neutrality equation

$$\sum_a \left[\int d^2v J_0 f_a + \frac{e_a}{m_a}\,\nabla_\perp \frac{n_{a0}}{B^2}\,\nabla_\perp \phi\,(x) + \frac{3e_a v^2_{th,a} e_{a0}}{4m_a \Omega^4_a}\,\nabla^4_\perp \phi(x)\right] = 0 \tag{8}$$

and the gyro-kinetic moment equation:

$$\begin{aligned} &-\frac{\partial}{\partial t}\frac{e}{m}\nabla_\perp \frac{n_0}{B^2}\nabla_\perp \phi + \nabla A_{||} \times b \cdot \nabla\left(\frac{\nabla \times B}{B}\right) + (B \cdot \nabla)\frac{(\nabla \times \nabla \times A) \cdot B}{B^2} \\ &= -\sum_a e_a \int v_d \cdot \nabla J_0 f_a d^3v + \frac{c}{v^2_{a0}}\,\frac{3v^2_{th,a}}{4\Omega^2_a}\nabla^3_\perp \frac{\partial \phi(x)}{\partial t} + \\ &B \cdot \nabla\left(\frac{4\pi e^2_a n_{a0} v^2_{th,a}}{2Bm_a c^2 \Omega^2_a}\,\nabla^3_\perp A_{||}\right) + B \times \nabla\left(\frac{2\pi e_a n_{0a} v^2_{th,a}}{B\Omega_a}\right) \cdot \nabla\nabla^2 \phi \end{aligned} \tag{9}$$

Here, Σ_a indicates the sum over different particle species with the perturbed distribution function f_a, mass m_a, charge e_a, unperturbed density n_{a0}, thermal velocity $v_{th,\,a} = \sqrt{T_a/m_a}$ and cyclotron frequency Ω_a. In the same simple limit as described above, carrying out the velocity space integrals and using $A_{||} = c(\nabla\psi)_{||}/iw$, these equations can be reduced to:

$$\phi - \psi = r^2_{LT}\,\nabla^2_\perp \phi \tag{10}$$

and

$$\nabla_\perp \cdot \frac{w^2}{v^2_A}\,\nabla_\perp \phi + \frac{\partial}{\partial s}\,\nabla^2_\perp \frac{\partial \psi}{\partial s} = 0 \tag{11}$$

leading, by elimination of ψ, to exactly the same fourth order equation as given above in equations (4) and (6). It should be noted however, that r_{LT} is not the same as $\hat{r}_{LT}$: the physics connected with parallel electric fields and collisions (Landau damping, finite banana orbit effects) would appear on the left hand side of Eq.(10) resp. right hand side of Eq.(11) originating from the exact kinetic integrals over the velocity space.

The contact between the gyro-kinetic model and the reduced kinetic model [22] is thus established.

3. MODEL

The basic version of Ligka [12] solves equations (8), (9) and the linear gyro-kinetic equation for the perturbed distribution function f up to 2nd order in $k_{\perp\rho i}$. The nite element discretisation scheme used is based upon using Hermite polynomials in the radial direction (with usually 100 to 200 grid points along the minor radius) and a Fourier decomposition in the poloidal angle. There is no coupling in the toroidal angle. Using a Galerkin method an eigenvalue problem is formed. The boundary conditions are chosen as $\phi_m(0) = \phi_m(a) = \psi_m(0) = \psi_m(a) = 0$. Straight field line coordinates for the background quantities given by the equilibrium code Helena [24] are chosen. Since the velocity space integrals depend on the eigenfrequency w in a complicated way (resonance integrals), the eigenvalue problem is nonlinear and Ligka uses the Nyquist contour integration technique to find the eigenvalues.

Ligka has been extended to calculate correctly the residual part of the Landau-type integrals for the case of negative growth rates, i.e. damped modes. It uses a rational interpolation scheme for the resonance denominator which allows for accurate and fast evaluation of the pole contributions without employing derivatives. Grid refinement techniques are also applied for the velocity space integration.

To be able to study the complex physics that is caused by non-ideal e ects in and near the gap region, Ligka has further been modified:

When examining the rich spectrum around a gap, many closely spaced modes are expected. Using a Nyquist solver is cumbersome under these conditions because many poles require a high number of sample points along the integration contour, even when background phase removal techniques are also applied [25]. Thus an antenna-like version of Ligka was developed: A drive vector is added to the right hand side of the homogeneous equation:

$$M(\omega)\begin{pmatrix} \dot{c} \\ \psi \end{pmatrix} = d \tag{12}$$

where **d** is only nonzero for the last finite element at the plasma edge, prescribing a small perturbation from the outside. The absolute value of **d** is chosen somewhat arbitrarily, however, it was tested

that different choices of **d** did not change the basic properties of the response spectrum, i.e. the location and the width of the peaks. The wave equations in the vacuum region and the proper boundary conditions are not implemented in this simple model.

The eigenfunctions are found by inverting $M(w)$ resulting in:

$$I \begin{pmatrix} \dot{c} \\ \psi \end{pmatrix} = M(\omega)^{-1} d, \tag{13}$$

and the plasma response is 'measured' by an integral over the eigenfunction:

$$R = \bullet_{m} \int_{0}^{a} \dot{c}_m \dot{c}_m^* dr \tag{14}$$

RESULTS

In the following, three different equilibria are used, all are based on the JET Pulse No: 42979 at 10.121*s* [26]. One of them is simplified to be up-down symmetric in order to create a case where the gaps are not aligned and single KTAEs can be found (equilibrium I). The other two equilibria differ only in a non-zero (equilibrium II) and a zero (equilibrium III) edge density. The basic parameters are $B = 3.53T$, $n_e(0) = n_i(0) = 3.72 \quad 10^{19} m^{-3}$, $T_e(0) = T_i(0) = 2.94$keV, $q_0 = 0.87$ and $q_a = 3.5$. The profiles are shown in Figs.1 and 2.

The first test is carried out for just two harmonics (equilibrium I) that form a continuum gap as shown in Fig.3. The TAE is located within the gap at $s = 0.77$ and intersects the continuum at $s = 0.95$. In the ideal MHD case, one would find a spike in the eigenfunction due to the singularity of the ideal operator. With the fourth order term present, this singularity is resolved [22, 23] and an inwards propagating KAW wave is found (Fig.4).

Taking into account three poloidal harmonics removes the intersection with the continuum and opens the gap throughout the whole plasma for equilibria I and II (Fig.5) whereas the zero edge density of equilibrium III closes the gap near the edge. A frequency scan throughout the gap for the up-down symmetric case (equilibrium I) is shown in Fig.6. One can clearly see the position of the TAE at $w = 0.35 w_A$ and the onset of the KTAEs at about $w = 0.52 w_A$. The KTAEs are generated by two KAWs that propagate towards each other and form a standing wave between the two continuum intersections at a given frequency. For increasing frequency the two intersection layers move away from each other, allowing for more and more maxima in between, as shown in Fig.7. The first 4 KTAEs with 'quantum numbers' $p = 0, 1, 2, 3$ are shown in this plot.

Similarly, on the lower side of the gap, two KAWs at the continuum intersections are also excited.

In contrast to the KTAE case above, the waves do not superpose since they are propagating away from each other (Fig. 8).

When the equilibrium II is analysed, a more complicated situation arises because the m = 1, m = 2 gap and the m = 2, m = 3 gap are more aligned, leading to a multiple KTAE structure as shown in Fig.9. One can clearly see a p = 0 mode in the m = 1, m = 2 gap and a p = 1 mode in the m = 2, m = 3 gap.

For all three equilibria, a global TAE within the gap can easily be identi ed. In order to find their damping rates, the Nyquist-solver-version of Ligka was employed since the present antenna version uses some simplifications in the kinetic integrals to allow for fast frequency scans. (An antenna version with all kinetic effects retained could, of course, also be employed, and the damping rates determined from the width of the response peaks. A future, parallelised version of the antenna version will use this approach.) The sampling contours were chosen to be relatively small since the approximate real eigenvalue was known from the antenna spectrum. Usually 32 to 64 sampling points were required to obtain a converged solution. The code is parallelised over the radial direction for solving the velocity space integrals. A typical run for three harmonics and 200 radial grid points took 10 hours on a 16 processor (2.8GHz) Linux cluster.

In the case of equilibrium II the damping rate was found to be 0.14% with contributions from circulating particles only. Including trapped particles increased the value to 0.24%. This is still too small compared to the experimental value of 2% [7]. However, since the errors on the density measurements are relatively large, especially at the plasma edge, one cannot be sure that the gap is really open. In the presence of a closed gap (equilibrium III) the calculated damping rate goes up to 0.65% for three poloidal harmonics, and up to 0.70% for five harmonics, which is expected to be close to the converged value since higher order harmonics change the result only by roughly an order $\in$. Figure 10 shows the global eigenfunction for this case. One can see that near the edge a KAW is excited. No mode conversion in the centre was found.

The eigenmode structure in all of these cases does not show any significant influence due to radiative damping because the non-ideal parameter λ is relatively small: $\lambda = 0{:}037$. The gyro-radius is about 2.0mm and the shear is 1.4 at the centre of the gap. However, under certain experimental conditions (lower magnetic field, higher temperatures, higher shear) λ can be up to 10 times larger. In this case, KAWs may strongly ‘tunnel’ towards the TAE, resulting in mode structures such as given in Fig.11. The damping rates in such cases (e.g. Pulse No: 52206@22.9s) can be as high as 1%. Detailed analysis and also comparisons with measured mode structures will be reported in a future paper.

CONCLUSIONS AND OUTLOOK

It has been shown that the gyro-kinetic formulation used in the Ligka code recovers the reduced kinetic model and is therefore applicable to the physics of kinetically modified global shear Alfvén modes. An antenna-like version allows the identification of all modes in a given frequency range,

such as in and around the TAE gap. With this information, the damping rates of TAEs with and without a closed gap (due to finite or zero edge density) can be determined. For the JET pulse with an open gap, Pulse No: 42979@10.121*s*, the calculated damping rates are still about a factor of 8 too small, with a closed gap only about a factor of 4. In the case of an open gap, no significant mode conversion at the edge has been found, in agreement with the results in Ref. [11] and in contrast with Ref. [9]. The reason for this could be differing plasma-edge boundary conditions [11] and that the damping rates in Ref. [9] are given for externally driven modes modelling the JET antenna system, whereas the damping rates presented in this papers are eigenfunctions of the plasma part only. For a closed gap, in agreement with Refs. [9, 11], continuum damping at the edge was found to be the strongest damping mechanism. No mode conversion in the plasma centre was found in contrast to [7, 27].

The remaining discrepancies will be further investigated, especially the sensitivity of the damping rates due to the edge boundary conditions. Further benchmarks with analytical, semi-analytical and other numerical models will be carried out.

In situations where the non-ideal parameter is large, modi cations of the TAE due to tunnelling can be seen. This confirms that only self-consistent models such as the Ligka code can be applied, resulting in damping rates up to 1%.

REFERENCES

[1]. C.Z. Cheng, L. Chen, M.S. Chance, Annals of Physics **161**, 21 (1985)

[2]. C.Z. Cheng, M.S. Chance, Phys. Fluids **29**, 11 (1986)

[3]. G.Y. Fu, J.W. VanDam, Phys. Fluids **1**, 1949 (1989)

[4]. R.R. Mett, S.M. Mahajan, Phys. Fluids B **4**, 2885 (1992)

[5]. D. Borba, W. Kerner, J. Comput. Phys **153**, 101 (1999)

[6]. G.Y. Fu, C.Z. Cheng, R. Budney, Z. Chang, D.S. Darrow, E. Fredrickson, E. Mazzucato, R. Nazikian, K.L. Wong, and S. Zweben, Phys. Plasmas **3**, 4036 (1996)

[7]. A. Fasoli, A. Jaun, D. Testa, Phys. Lett. A **265**, 288 (2000)

[8]. D. Testa, G.Y. Fu, A. Jaun, A. Fasoli, O. Sauter and JET-EFDA contributors, Nucl. Fusion **43**, 479 (2003)

[9]. D. Borba, H.L. Berk, B.N. Breizman, A. Fasoli, F. Nabais, S.D. Pinches, S.E. Sharapov, D. Testa and JET-EFDA contributors, Nucl. Fusion **42**, 1029 (2002)

[10]. A. Jaun, K. Appert, J. Vaclavik and L. Villard, CPC **92**, 153 (1995)

[11]. G.Y. Fu, H. L. Berk, A. Pletzer, Phys. Plasmas **12**, 082505 (2005)

[12]. Ph. Lauber, 'Linear Gyrokinetic Description of Fast Particle Effects on the MHD Stability in Tokamaks', Ph.D. Thesis, TU München, (2003)

[13]. H. Qin, 'Gyrokinetic Theory and Computational Methods for Electromagnetic Perturbations in Tokamaks', Ph.D. Thesis, Princeton University (1998)

[14]. H. Qin,W.M. Tang, G.Rewoldt, Phys. Plasmas **5**, 1035 (1998)

[15]. S. D. Pinches, ‘Nonlinear Interaction of Fast Particles with Alfvén Waves in Tokamaks’, Ph.D. Thesis, The University of Nottingham (1996)
[16]. S. D. Pinches, L.C. Appel, J. Candy *et al.*, CPC **111**, 131 (1998)
[17]. H.L Berk, R.R. Mett, and D.M. Lindberg, Phys. Fluids B **5**, 3969 (1993)
[18]. H.M. Rosenbluth, H.L Berk, J.W. Van Dam, and D.M. Lindberg, Phys. Rev. Lett, **68**, 596 (1992)
[19]. J. Candy, M.N. Rosenbluth, Phys. Plasmas **1**, 356 (1994)
[20]. H.L. Berk, J.W. Van Dam, Z. Guo, and D.M. Lindberg, Phys. Fluids B **4**, 1806 (1992)
[21]. B.N. Breizman, S.E. Sharapov , Plasma Phys Control. Fusion **37**, 1057 (1996)
[22]. A. Hasegawa, L. Chen, Phys. Rev. Lett. **35**, 370 (1975)
[23]. A. Hasegawa, L. Chen, Phys. Fluids **19**, 1924 (1976)
[24]. G.T.A. Huysmans. J.P. Goedbloed, W. Kerner, Proc. CP90 Conf. on Comp Phys.Proc., World Scientific Publ.Co., p. 371 (1991)
[25]. S. Brunner, private communication (2001)
[26]. A. Jaun, private communication (2004)
[27]. A. Jaun, A. Fasoli, J. Vaclavik and L. Villard, Nucl. Fusion **39**, 2095 (1999)

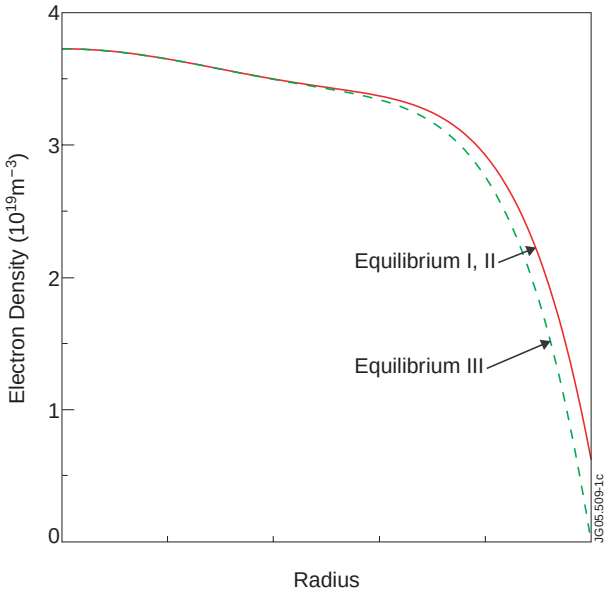

Figure 1: Density profiles for equilibria I, II and III.

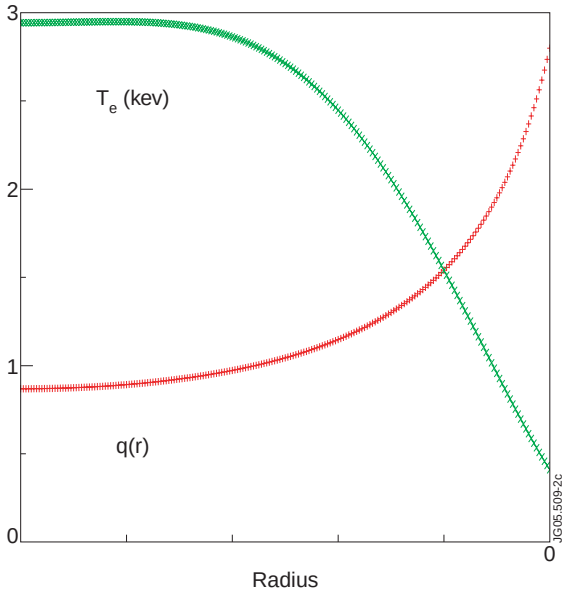

Figure 2: Safety factor and electron temperature profile for equilibria I, II and III.

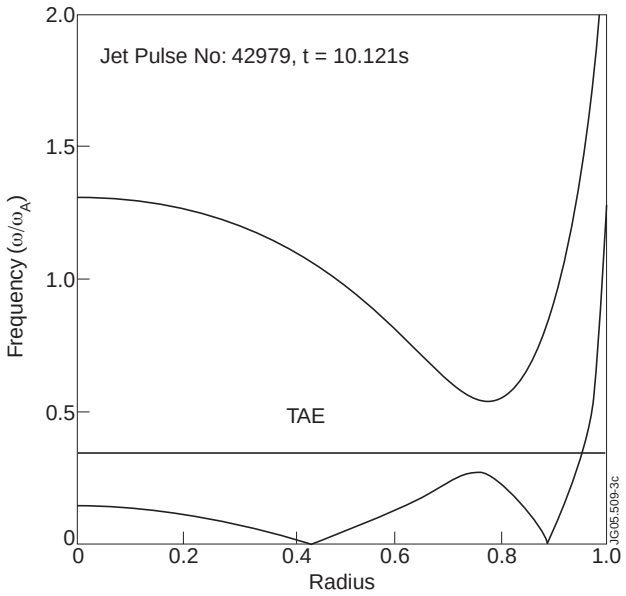

Figure 3: Shear Alfvén continuum for two poloidal harmonics, up-down symmetric equilibrium I.

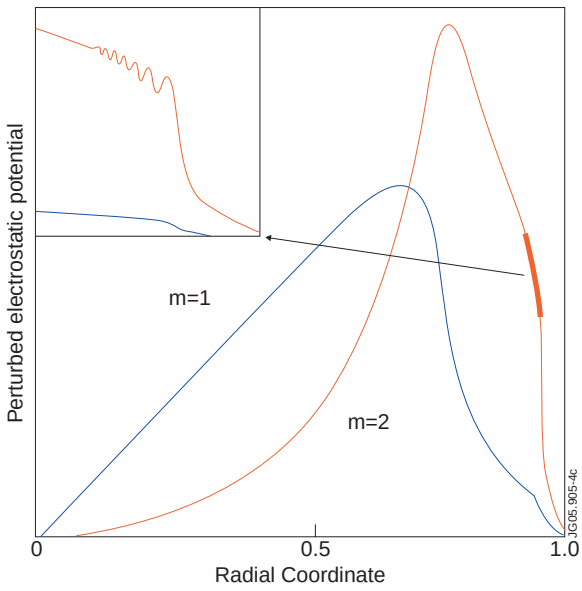

Figure 4: Eigenfunction of a global TAE that intersects the continuum at r ≈ *0.94 exciting an inwards propagating KAW.*

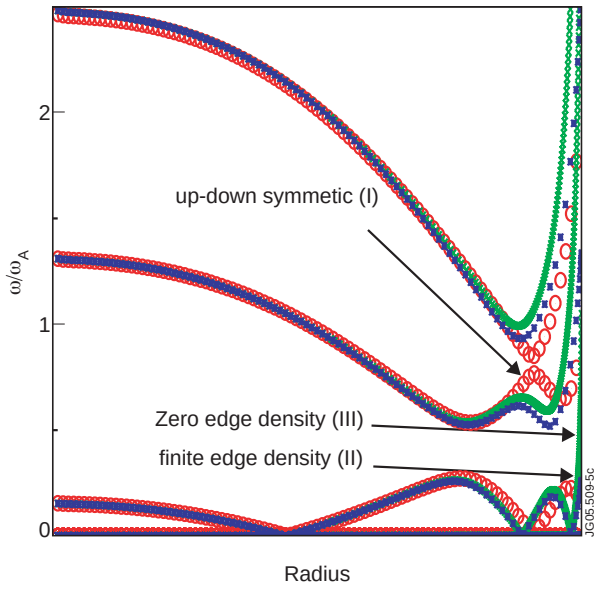

Figure 5: Shear Alfvén continuum for three poloidal harmonics for equilibria I,II and III.

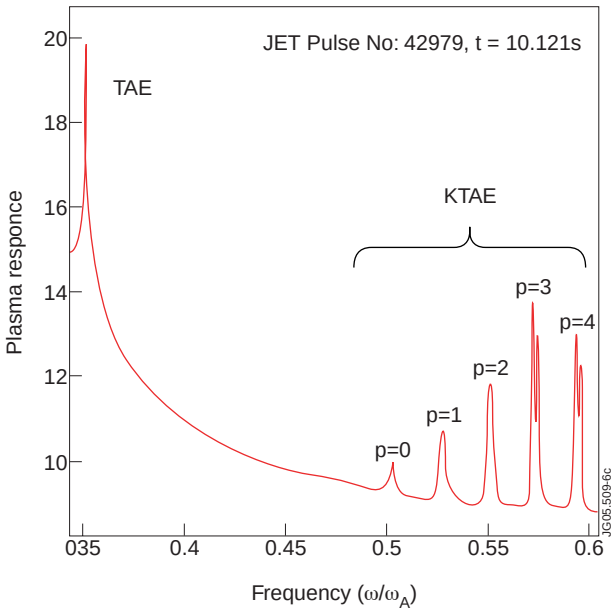

Figure 6: Calculated antenna response Log(R) *as function of an externally applied frequency for equilibrium I.*

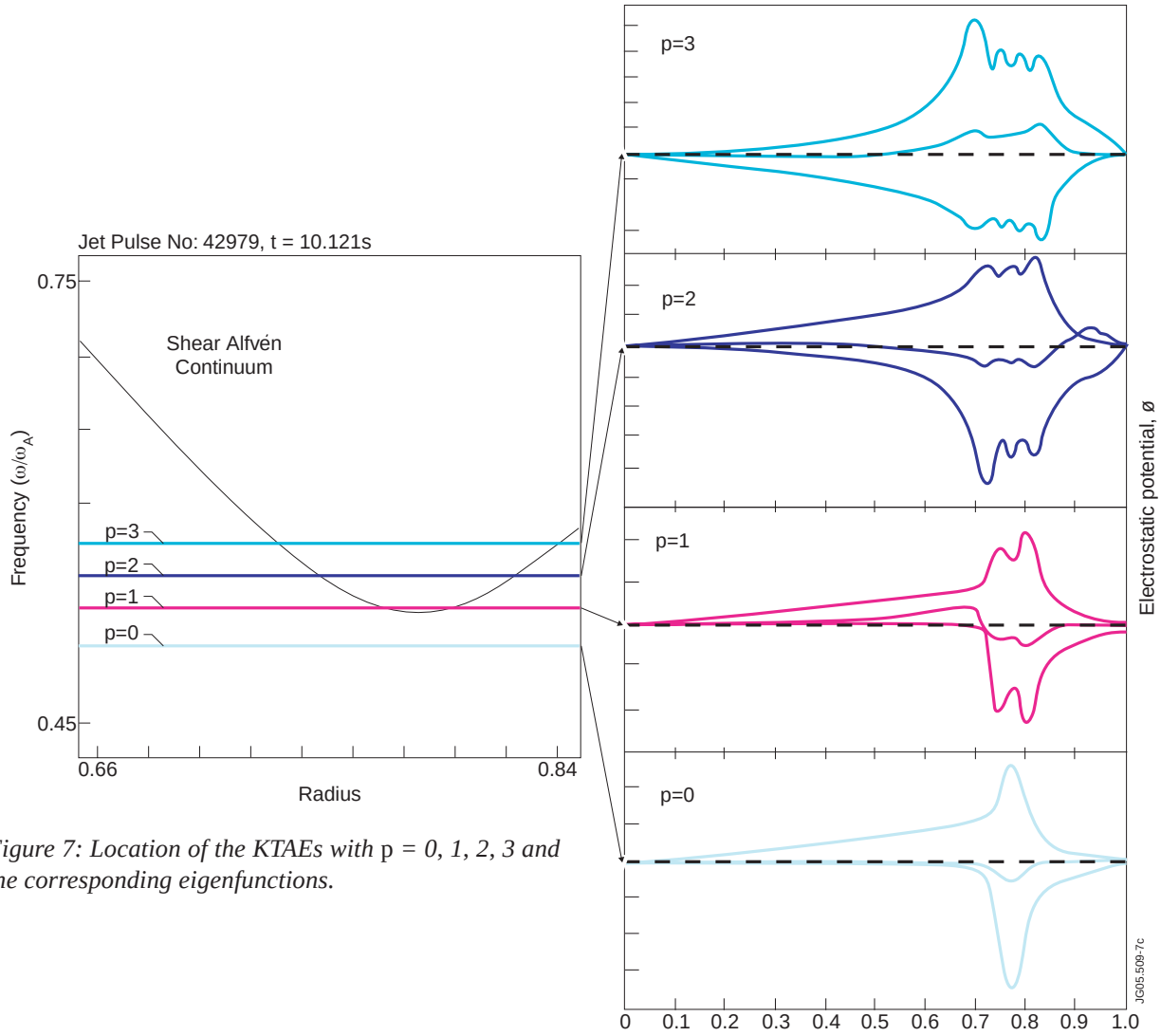

Figure 7: Location of the KTAEs with p = *0, 1, 2, 3 and the corresponding eigenfunctions.*

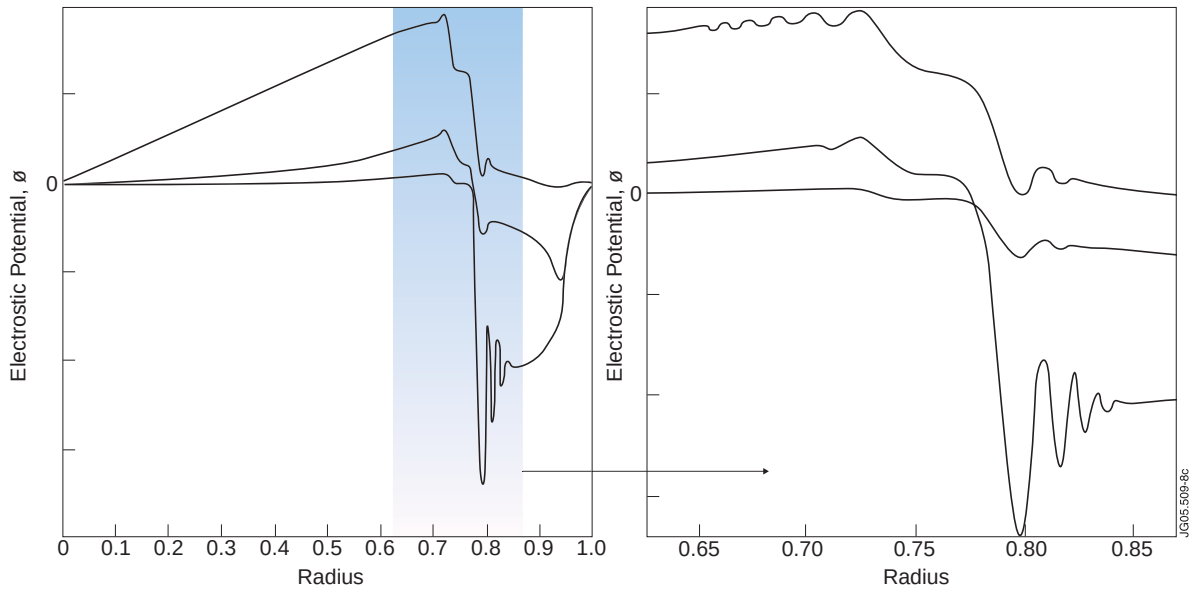

Figure 8: Eigenfunction of a mode located below the lower gap boundary ($\omega = 0.24\omega_A$*).*

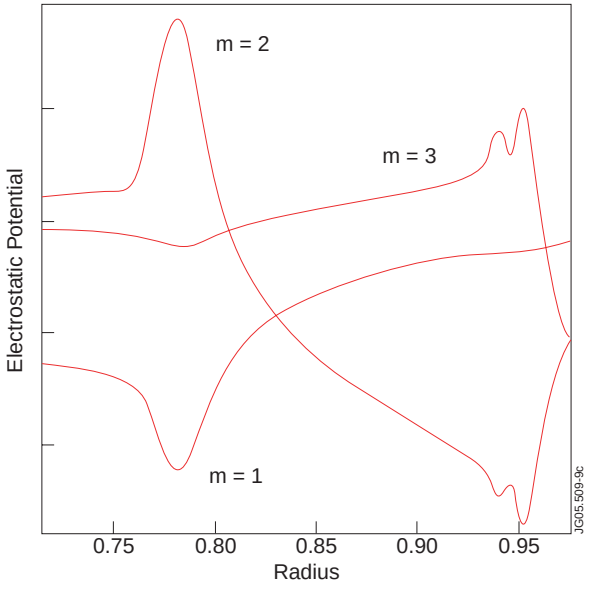

Figure 9: Eigenfunction of a multiple gap KTAE at $\omega = 0.518\omega_A$*, equilibrium II.*

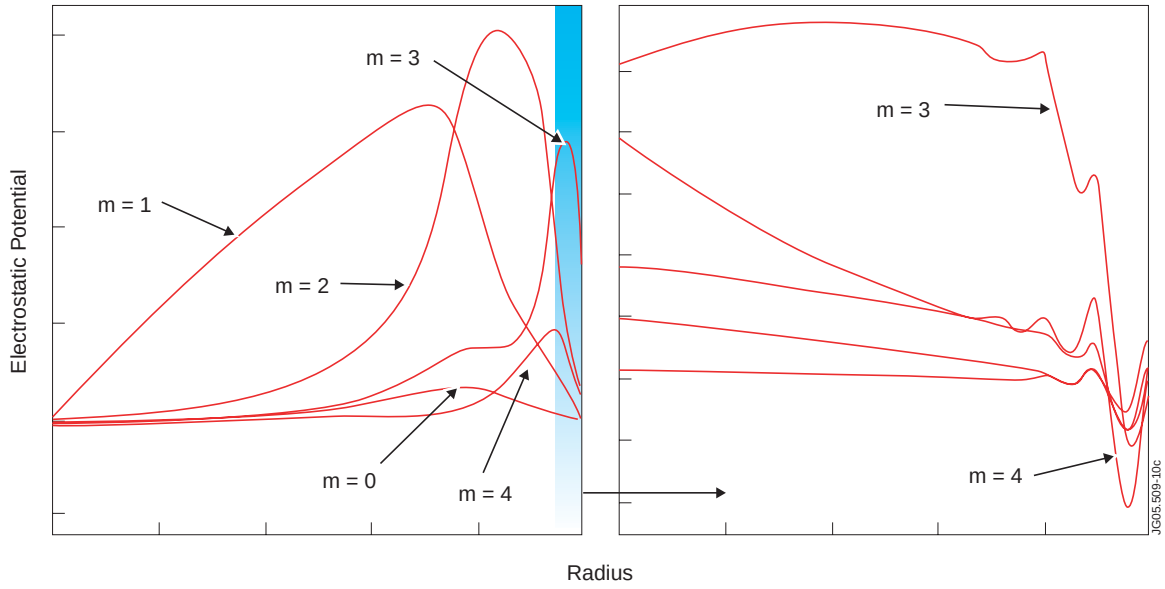

Figure 10: Eigenfunction of a global TAE with a closed gap with $\omega = 0.345\omega_A$ *and* $\gamma/\omega = 0.7\%$ *(equilibrium III).*

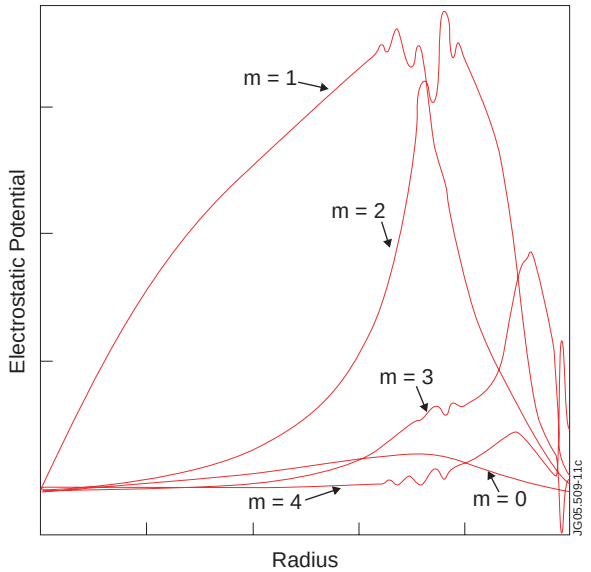

Figure 11: Eigenfunction of a global TAE (Pulse No: 52206@22.9s) in the presence of a large non-ideal parameter $\lambda \approx 0.3$, $\gamma/\omega = 1.25\%$.